# Analysis of the Magnetic Properties of RFe$_{11}$Ti and RFe$_{11}$TiH (R=Tb,Ho)

S. W. Xu[1], Y. Yan[1,2*], H. M. Jin[1], X. F. Wang[1], W. Q. Wang[1], and F. Su[1]

*[1]Department of Physics, Jilin University, Changchun 130023, P.R. China*
*[2]State Key Laboratory for Superhard Materials, Jilin University, Changchun 130023, P.R. China*

The values of crystalline-electric-field parameters $A_{nm}$ for RFe$_{11}$TiH$_x$ (R=Tb,Ho) (x=0,1) are obtained by fitting calculations to the magnetization curves along the crystal axes at 4.2 K and higher temperatures. The insertion of H element in RFe$_{11}$Ti significantly affects CEF parameters $A_{nm}$. By using exchange field $2\mu_B H_{ex}$ derived by inelastic neutron scattering and fitted $A_{nm}$, the calculations reproduce the experimental curves well.

**Key words :** crystalline-electric-field, rare-earth 3d metal compound, magnetization curve

## 1. Introduction

During the last few years, the magnetic properties of the intermetallic compounds RFe$_{11}$Ti and their hydrides RFe$_{11}$TiH have been studied extensively [1-8]. Many experimental investigations of the intrinsic magnetic properties of RFe$_{11}$TiH$_x$ (x=0,1) single crystals have been reported [1-7]. The insertion of hydrogen element in RFe$_{11}$Ti significantly changes their Curie temperature, saturation magnetization and magnetic anisotropy. Nikitin et al evaluated the values of Ho-Fe exchange field $2\mu_B H_{ex}$ and crystalline-electric-field (CEF) parameters $A_{nm}$ in HoFe$_{11}$TiH$_x$(x=0,1) by fitting calculations to the magnetization curves along the crystal axes at 4.2 K and concluded that hydrogenation leads to the increase in $2\mu_B H_{ex}$ of about 10% [1]. Inelastic neutron scattering (INS) experiments on RFe$_{11}$Ti and RFe$_{11}$TiN (R=Gd,Er) show that insertion of N element leads to the decrease in $2\mu_B H_{ex}$ of about 14% [9]. INS experiments on Gd$_2$Fe$_{17}$ and Gd$_2$Fe$_{17}$M$_x$ (M: C, N, D (deuterium)) also show that insertion of light interstitial element (C, N, D) reduces the Gd-Fe exchange field at Gd site in Gd$_2$Fe$_{17}$ [10]. In this connection, the insertion of light interstitial elements leads to the enhancement of Curie temperature and the lattice expansion of the compounds.

This work is to evaluate the values of CEF parameters $A_{nm}$ of RFe$_{11}$TiH$_x$ (R=Tb,Ho) (x=0,1) from the experimental magnetization curves at 4.2 K and higher temperatures on

the basis of the single-ion model and analyse the experimental data.

## 2. Method of Analysis

RFe$_{11}$TiH$_x$ (x=0,1) have a ThMn$_{12}$-type tetragonal structure with space group I4/mmm. There is one rare-earth ion site with the point symmetry D$_{4h}$. The Hamiltonian of the rare-earth ion consists of the CEF interaction, the R-Fe exchange interaction and the Zeeman energy, i.e.

$$H=H_{CEF}+2\mu_B \vec{S} \bullet \vec{H}_{ex}+\mu_B(\vec{L}+2\vec{S}) \bullet \vec{H}, \qquad (1)$$

In the coordinate system with $x$ and $z$ axes along the [100] and [001] axes, respectively, the CEF interaction can be expressed as

$$H_{CEF}= \sum_{n=2,4,6} A_{n0} \sum_{j} C_{n0}(\theta_j, \varphi_j)$$
$$+ \sum_{n=4,6} A_{n4} \sum_{j} (C_{n4}(\theta_j, \varphi_j)+C_{n-4}(\theta_j, \varphi_j)), \qquad (2)$$

Here

$$C_{nm}(\theta_j, \varphi_j)=[4\pi/(2n+1)]^{1/2} Y_{nm}(\theta_j, \varphi_j), \qquad (3)$$

$Y_{nm}(\theta_j, \varphi_j)$ are the spherical harmonics, $\theta_j$ and $\varphi_j$ are the polar and azimuthal angles of the position vector of jth 4f electron. It is assumed that the rare-earth ion is trivalent and $\vec{H}_{ex}$ is proportional to the magnetic moment of the Fe sublattice $\vec{M}_{Fe}$. The matrix elements of Eq. (1)

*Corresponding author: Tel: +86-0431-8499047,
e-mail: jhm@mail.jlu.edu.cn

are calculated by using the irreducible-tensor-operator technique. For a given applied field $\vec{H}$ and a direction of $\vec{H}_{ex}$, the eigenvalues $E_i$ and eigenfunctions $|n_i\rangle$ ($i = 1, 2, \cdots, 2J+1$) are obtained by diagonalizing the $(2J+1) \times (2J+1)$ matrix. The free energy for $RFe_{11}TiH_x$ (x=0,1) is given by

$$F(\vec{H}, \vec{M}_{Fe}, T) = -kT\ln Z + K_1(T)Sin^2\theta_{Fe} - \vec{M}_{Fe}(T) \cdot \vec{H},$$
(4)

Where

$$Z = \sum_i \exp(-E_i/kT),$$
(5)

and $K_1(T)$ is the magnetocrystalline anisotropy constant of the Fe sublattice. $M_{Fe}(T/T_C)/M_{Fe}(0)$ and $K_1(T/T_C)/K_1(0)$ for $RFe_{11}Ti$ and $RFe_{11}TiH$ are taken to be same as those for $LuFe_{11}Ti$ and $LuFe_{11}TiH$, respectively [4]. The value of $M_{Fe}(0)$ is taken to be 20.1 $\mu_B/f.u.$ for $RFe_{11}Ti$ and 20.6 $\mu_B/f.u.$ for $RFe_{11}TiH$, respectively. $K_1(0)=23.6$ K/f.u. for $RFe_{11}Ti$ and $K_1(0)=26.6$ K/f.u. for $RFe_{11}TiH$ is same as that for $LuFe_{11}Ti$ and $LuFe_{11}TiH$, respectively [4]. The equilibrium direction of $\vec{M}_{Fe}$ is determined from minimization of $F(\vec{H}, \vec{M}_{Fe}, T)$, and the magnetic moments of the rare-earth ion and of $RFe_{11}TiH_x$ (x=0,1) are given by

$$\vec{M}_R = -\mu_B \sum_i \langle n_i|\vec{L} + 2\vec{S}|n_i\rangle \exp(-E_i/kT)/Z,$$
(6)

$$\vec{M} = \vec{M}_R + \vec{M}_{Fe}.$$
(7)

The value of the exchange field $2\mu_B H_{ex}$ in $RFe_{11}TiH_x$ (R=Tb,Ho) (x=0,1) were estimated as follows. The value of $2\mu_B H_{ex}(T \approx 20$ K) derived by INS experiment is about 470 K, 343 K and 250 K for $SmFe_{11}Ti$ [11], $GdFe_{11}Ti$ [9] and $ErFe_{11}Ti$ [9]. It is known that the value of $2\mu_B H_{ex}$ decrease monotonically across the rare-earth series from Pr to Er in many Rare-earth-Fe intermetallic compounds [12, 13]. By extrapolating the value for $SmFe_{11}Ti$, $GdFe_{11}Ti$ and $ErFe_{11}Ti$ according such a variation in $2\mu_B H_{ex}$ across the $RFe_{11}Ti$ series, the value of $2\mu_B H_{ex}(T \approx 20$ K) for $TbFe_{11}Ti$ and $HoFe_{11}Ti$ is estimated to be about 285 K and 260 K, respectively. It is assumed that the decrease of $2\mu_B H_{ex}$ induced by insertion of N element is about five times of the decrease by insertion of H in $RFe_{11}Ti$ as in $R_2Fe_{17}$ compounds [10]. The value of $2\mu_B H_{ex}(T \approx 20$ K) for $TbFe_{11}TiH$ and $HoFe_{11}TiH$ is estimated to be about 277 K and 253 K.

The values of CEF parameters $A_{nm}$ were evaluated by fitting calculations to the magnetization curves at 4.2 K and higher temperatures for the single crystals of $RFe_{11}TiH_x$ (R=Tb,Ho) (x=0,1).

## 3. Results and Discussion

Table 1 lists the fitted values of CEF parameters $A_{nm}$. It can be seen that the value of $A_{20}$ of $RFe_{11}TiH$ increase about 77%~113% towards negative value compared with that of corresponding $RFe_{11}Ti$. In this connection, a Mössbauer study of [155]Gd in $GdFe_{11}TiH_x$ (x=0,1) has shown that hydrogenation leads to about 53% increase of the electric field gradients at Gd ion site, which are proportional to $A_{20}$ [8]. Hydrogenation has also significant effect on the high-order CEF parameters $A_{nm}$. The significant changes of $A_{nm}$ cause the change of magnetic aniso-

**Table 1.** The fitted values of CEF parameters $A_{nm}$

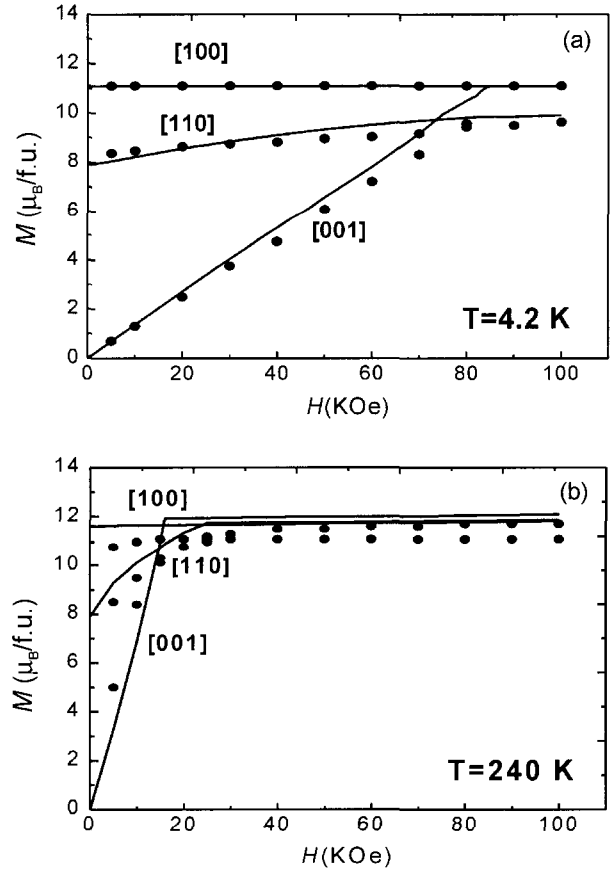| | $A_{20}$ | $A_{40}$ | $A_{44}$ | $A_{60}$ | $A_{64}$ |
|---|---|---|---|---|---|
| $TbFe_{11}Ti$ | -90 K | -4 K | -100 K | 2 K | -87 K |
| $TbFe_{11}TiH$ | -160 K | -110 K | 34 K | 20 K | -25 K |
| $HoFe_{11}Ti$ | -61 K | -122 K | -176 K | 432 K | -13 K |
| $HoFe_{11}TiH$ | -130 K | -85 K | -80 K | 62 K | -10 K |



**Fig. 1.** (a) magnetization curves of $TbFe_{11}Ti$ at 4.2 K: ● experimental data from [2]; —— calculation. (b) magnetization curves of $TbFe_{11}Ti$ at 240 K: ● experimental data from [6]; —— calculation.
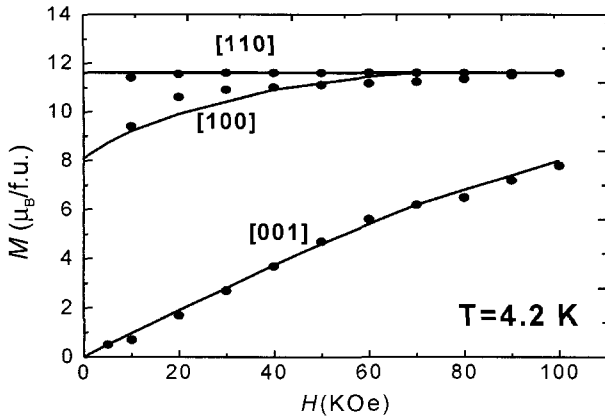
**Fig. 2.** magnetization curves of TbFe₁₁TiH at 4.2 K: ● experimental data from [2]; —— calculation.

tropy. For example, the change of the easy magnetization direction induced by insertion of H for TbFe₁₁Ti, which is from the [100] to the [110] axis, mainly originates from a sign change of $A_{44}$.
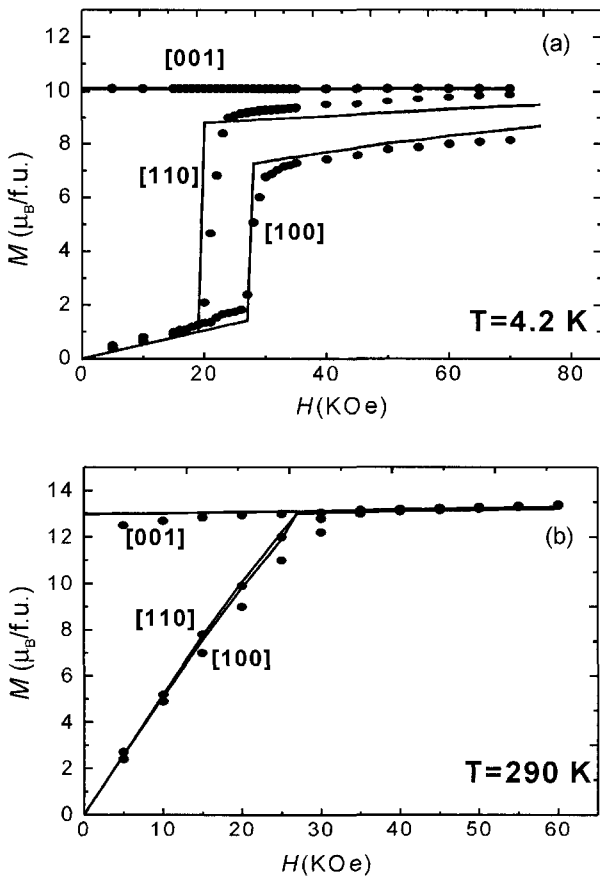
Fig. 1 to 4 show the comparison of the calculations with the experimental data. The symbols represent the experimental data, and the full curves the calculations. Fig. 1(a) and 1(b) show the magnetization curves along the [100], [110] and [001] axes at 4.2 K and 240 K for TbFe₁₁Ti. Fig. 2 shows the magnetization curves along the [100], [110] and [001] axes at 4.2 K for TbFe₁₁TiH. Fig. 3(a) and 3(b) show the magnetization curves along the [100], [110] and [001] axes at 4.2 K and 290 K for HoFe₁₁Ti. Fig. 4(a) and 4(b) show the magnetization curves along the [100], [110] and [001] axes at 4.2 K and 300 K for HoFe₁₁TiH. At 4.2 K, a field-induced first-order magnetization process (FOMP) in the [001] direction was found by our calculation for HoFe₁₁TiH. It may be as in the FOMP in the DyFe₁₁Ti [14] that a continuous increase of the magnetization instead of a discontinuous jump in the experimental curves is observed for magnetic field around the critical field. The predicted FOMP by calculation need to be confirmed by the singular-point-detection technique in HoFe₁₁TiH.
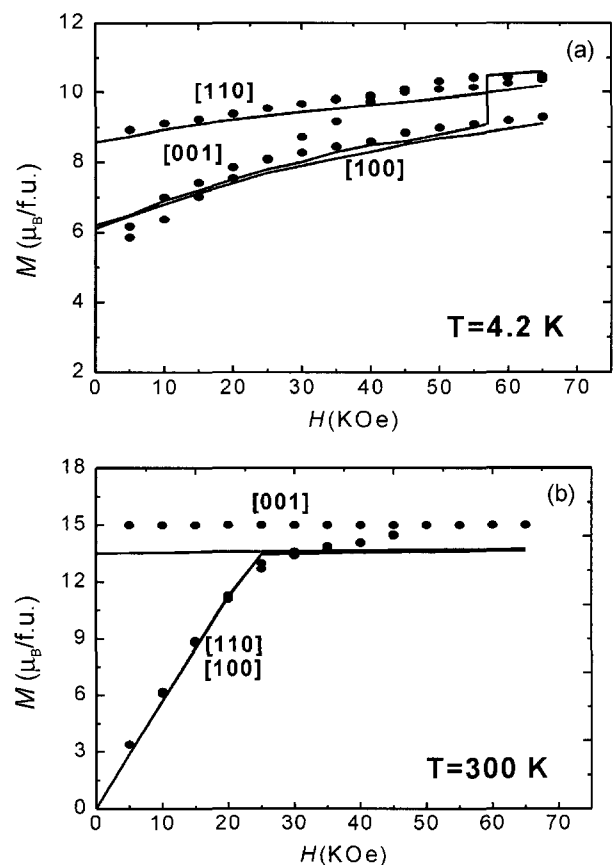


**Fig. 3.** (a) magnetization curves of HoFe₁₁Ti at 4.2 K: ● experimental data from [1]; —— calculation. (b) magnetization curves of HoFe₁₁Ti at 290 K: ● experimental data from [6]; —— calculation.



**Fig. 4.** (a) magnetization curves of HoFe₁₁TiH at 4.2 K: ● experimental data from [1]; —— calculation. (b) magnetization curves of HoFe₁₁TiH at 300 K: ● experimental data from [7]; —— calculation.

## Acknowledgements

## References

[1] S. A. Nikitin, I. S. Tereshina, N. Yu Pankratov and Yu V Skourski, Phys. Rev. B **63**, 35 (2001).

[2] S. A. Nikitin, I. S. Tereshina, V. N. Verbetsky, A. A. Salamova, and K. P. Skokov, J. Alloys Comp. **322**, 42 (2001).

[3] I. S. Tereshina, P. Gaczynski, V. S. Rusakov, H. Drulis, and S. A. Nikitin, J. Phys.: Condens. Matter. **13**, 8161 (2001).

[4] I. S. Tereshina, S. A. Nikitin, N. Yu Pankratov, G. A. Bezkorovajnaya, A. A. Salamova, V. N. Verbetsky, T. Mydlarz, and Yu. V. Skourski, J. Magn. Magn. Mater. **231**, 213 (2001).

[5] S. A. Nikitin, I. S. Tereshina, V. N. Verbetsky, and A. A. Salamova, J. Alloys Comp. **316**, 46 (2001).

[6] C. Abadia, P. A. Algarabel, B. Garcia-Landa, M. R. Ibarra, A. del Moral, N. V. Kudrevatykh, and P. E. Markin, J. Phys.:Condens. Matter. **10**, 349 (1998).

[7] S. A. Nikitin, I. S. Tereshina, Yu. V. Skourski, N. Yu Pankratov, K. P. Skokov, V. V. Zubenko, and I. V. Telegina, Physics of the Solid State **43**, 290 (2001).

[8] O. Isnard, P. Vulliet, J. P. Sanchez, and D. Fruchart, J. Magn. Magn. Mater. **189**, 47 (1998).

[9] D. P. F. Hurley, M. Kuzímin, J. M. D. Coey, and M. Kohgi, J. Magn. Magn. Mater. **140-144**, 1027 (1995).

[10] O. Isnard, A. Sippel, M. Loewenhaupt, and R. Bewley, J. Phys.:Condens. Matter **13**, 3533 (2001).

[11] O. Moze, R. Caciuffo, H. S. Li, B. P. Hu, J. M. D. Coey, R. Osborn, and A. D. Taylor, Phys. Rev. B **42**, 1940 (1990).

[12] E. Belorizky, M. A. Fremy, J. P. Gavigan, D. Givord, and H. S. Li, J. Appl. Phys. **61**, 3971 (1987).

[13] M. Loewenhaupt, and I. Sosnowska, J. Appl. Phys. **70**, 5967 (1991).

[14] B. P. Hu, H. S. Li, J. M. D. Coey, and J. P. Gavigan, J. Phys.: Condens. Matter **413**, 2221 (1990).